Kuwait J.Sci., Vol.50, No.(3A),July.2023,pp(1-12)

Carbon nanodots-based C-dips for rapid colorimetric detection of clinically important metal ions

Sumaira Nishat[1,2], Malik Wasim Abbas[1], Fazli Rabbi Awan[1, *], Razium Ali Soomro[1,3]

[1]Health Biotechnology Division, National Institute for Biotechnology and Genetic Engineering College, Pakistan Institute of Engineering and Applied Sciences (NIBGE-C, PIEAS), Faisalabad, Pakistan
[2] Dept. of Computer Science, University of Agriculture, Faisalabad, Pakistan
[3]Beijing Advanced Innovation Centre for Soft Matter Science and Engineering, Beijing University of Chemical Technology, Beijing, 100029, P.R. China

**Corresponding Author: awan.fr@gmail.com*

Abstract

Owing to unique physical and optical properties, fluorescent carbon dots (C-dots) are used in various biomedical applications. In this study, C-dots have been integrated as sensing agent on paper surface for colorimetric determination of clinically important analytes. Polyacrylamide-based C-dots coated C-dips showed visible color change from white to brown for iron (Fe^{2+}, Fe^{3+}) sample. Moreover, iron and copper (Cu^{2+}) samples showed significant quenching of C-dots under UV. Images captured with/without UV were analyzed to study the relationship between different iron and copper concentrations and colorimetric intensity values. Color intensity and fluorescence showed a linear relationship with concentrations of iron and copper (Range: 1×10^{-4} to 1×10^{-2} M, Linearity: $R^2 = 0.94$). LOD from the paper sensor showed a sensitivity of 3.89×10^{-5} µM, 4.65×10^{-5} µM and 6.7×10^{-5} µM for Fe^{3+}, Fe^{2+} and Cu^{2+} respectively, reflecting its reliability as low-cost sensing solution to analyze clinically relevant analytes as reported in current study.

Keywords: Carbon dots; copper; iron; nanotechnology; paper-based sensors.

1. Introduction

In the human body, different metabolic processes generate various products and by-products. The optimum concentration of these products or by-products is essential for maintaining human health. Dysregulation in any metabolic activity may affect the physiological mechanisms and homeostasis which regulate the concentration of different analytes like proteins, hormones, metabolites, metal and non-metal ions, etc. Changes in the production or levels of any analyte beyond a specific threshold may disturb the whole biological system and may lead to different life-threatening diseases, hence serve as a warning sign for the timely treatment of diseases of heart, kidney, liver, etc. For example, iron, being the major structural and functional element of hemoglobin, is responsible for the transport of oxygen. Similarly, copper is an important analyte to regulate many body functions as a cofactor. Change in iron or copper concentration may lead to various medical complications (e.g. anemia, Wilson disease) and may damage vital organs like heart, kidney, liver and brain, etc. So, monitoring the level of these metals is highly recommended to ensure a healthy state. Currently different traditional but sophisticated analytical techniques like Atomic Absorption Spectrometry, Voltammetry, Resonance Scattering Spectroscopy, Inductively Coupled Plasma Mass Spectrometry, Inductively Coupled Plasma Atomic Emission Spectrometry, Fluorescence Spectrometry, etc. are in use to detect and quantify these metal ions. Undoubtedly the results of these techniques are quite close to the actual analyte concentrations (selective and sensitive) but the associated shortcoming of these methods like the requirement for expensive instruments and reagents, laboratory infrastructure, time-consuming long protocols, need for professional experts to run such instruments, etc. render these choices unfavorable for resource-limited areas as in the developing countries, pandemics and emergencies (like accidents, natural disasters). Hence, there is a need to have a cost-effective, fast and feasible way to perform metal ion detection at the patient care site in the form of point-of-care testing (POCT) devices.

The extensive need for point-of-care (POC) diagnostics in resource-limited settings is a continuous motivation for researchers from interdisciplinary fields of science and technology to develop cost-effective, sensitive and highly selective diagnostic assays. In this context, the innovative concept of the microfluidic wax-printed paper-based diagnostic assay was introduced by the Whitesides group at the Harvard University in 2007 (Martinez *et al.*, 2008b; Martinez *et al.*, 2008a; Martinez *et al.*, 2007). Paper, being the cheap, easily available, easy to transport, modify and discard, has become one of the most favorite substrates to perform diagnostic assays. For the last decade or so, nanotechnology has strongly embedded its footprints in designing sensitive, selective and quantitative colorimetric on-site diagnostic assays for different diseases. Nanoparticles (NPs) ranging in size 1-100 nm are being employed in designing POC applications (Kumar *et al.*, 2014). Owing to their unique properties like Surface Plasmon Resonance (SPR), biocompatibility, size and shape-dependent physical and chemical properties; various nanomaterials like gold, silver, platinum, quantum dots are being used in different colorimetric assays for the detection of numerous analytes. The modifiable chemistry of NPs has urged the nanotechnologists to exploit nanoparticles for sensitive detection of different biologically and clinically significant analytes like proteins, nucleic acid, metal ions like iron, copper and mercury, etc. (Piyanan *et al.*, 2018; Lee *et al.*, 2018; Guo *et al.*, 2016; Chaiyo *et al.*, 2015; Gao *et al.*, 2015; Priyadarshini and Pradhan, 2017; Mirabi *et al.*, 2019). Recently luminescent carbon nanoparticles, including carbon dots, graphene quantum dots, are also being used independently or to complement colorimetric assays for ultra-sensitive and selective selection of target analyte with less response time and cost.

Carbon – an abundant natural element is being actively used in different fields like energy production, health, etc. In the past few years, carbon allotropes including fullerenes, graphene, carbon nanotubes, carbon dots have gained the attention of researchers due to their unique electrical, thermal and biocompatible properties. As an alternative to other expensive metal based quantum dots, carbon-based quantum dots (C-dots, carbon quantum dots or carbon nanoparticles), discovered in 2004 during purification of single-walled carbon nanotubes by Xu *et al.*, are under research as one of the best fluorescent carbon nanomaterial (Siqueira and Oliveira, 2017; Ye *et al.*, 2004).

C-dots are quasi-spherical particles with a diameter of less than 10 nm. These NPs exhibit incomparable optical properties, electrochemiluminescence emission properties, economically feasible synthetic material and procedure, excellent water solubility, photostability, biocompatibility, easy modification/functionalization, conductivity, high chemical stability, environment friendliness and low toxicity. These NPs are being tremendously explored in different applications like bio-imaging, nano-medicine, catalysis, optoelectronics, energy conversion/storage and biosensing applications such as ions (Fe^{+3}, K^{+}, Cr^{+6}, Pb^{+2}, Zn^{+2} and Ag^{+}), small molecules, macromolecules, cell and bacteria (Zhao *et al.*, 2015; Namdari *et al.*, 2017; Sun and Lei, 2017; Tuerhong *et al.*, 2017; Adnan *et al.*, 2019; Nishat *et al.*, 2019; Mirabi et al., 2019). In one study, C-dots-based strip has been fabricated using screen-printed carbon electrode for Fe^{3+} detection in aqueous sample, wherein the C-dots (Diameter: 1-7 nm) were synthesized from carbon rods of used battery. The LOD of this strip was reported to be 0.44 ppm (Tan *et al.*, 2017). In another study, C-dots-based fluorescent chemosensor (Diameter: 4.5 nm) has been proposed for detection of Fe^{3+} in aqueous solution with LOD of 3.8 Mm. In this study, glutamic acid and ethylenediamine were used as reactants to synthesize C-dots (Chen *et al.*, 2020). Based on blue fluorescent property, nitrogen-doped carbon dot, prepared using N-(2-hydroxyethyl) ethylenediamine triacetic acid (HEDTA), have also been proposed for Fe^{3+} screening (Shah *et al.*, 2019). In another study, C-dots codoped with nitrogen and sulfur (Diameter: ~5 nm) were synthesized using citric acid (precursor) and thiourea (dopant), and proposed for Fe^{3+} sensing with LOD of 0.16 μM (Chan *et al.*, 2019).

In this study, we proposed a simple method to utilize carbon nanodots (C-dots, size: 10-20 nm) as sensitive colorimetric identifiers for iron and copper ions. The C-dots were synthesized by hydrothermal technique using PAM as a precursor while XRD, Raman and XPS confirmed their surface configuration and compositional suitability. The nanodips (spherically cut-Whatman-1 filter paper) were later soaked into C-dots with color change measurement that was carried using pixel intensity analysis using ImageJ software. The prepared C-dips could successfully identify the presence of said metal ions with a color change from white to brown, whereas quantification can be effectively carried out under UV-light, where the marked difference in color intensity could enable sensitive analytical quantification of clinically important metal ions.

2. Methodology

2.1 Chemicals

In this study, analytical grade reagents were used as received i.e. without additional treatment or purification while pure Milli-Q water was used for solution preparation. Ferric chloride ($FeCl_3$), ferrous chloride ($FeCl_2$) and polyacrylamide (PAM) were purchased from Sigma-Aldrich.

2.2 Instruments

UV–Visible spectroscopy (Lambda 35, PerkinElmer), X-ray Photoelectron spectroscopy (XPS) (ESCA200 spectrometer), Fourier transform infrared (FTIR) spectroscopy (Nicolet 5700, Thermo), transmission electron microscopy (TEM) (Jeol JEM 1200 EX MKI), X-ray diffraction (XRD) (model D-8, Bruker), electronic weighing balance (Metler Toledo), Magnetic Stirring Plate (MSP), vortex mixer (Hedolf Reax), double deionizer (Millipore), pH meter (Inolab, WTW series), UV-6 S/L (Herolab). The colorimetric output of the C-dots, with/without UV, was captured using 18-megapixel digital camera.

2.3 Synthesis of carbon dots

C-dots were synthesized using a one-pot hydrothermal method, wherein PAM was as a carbon precursor (Tuerhong *et al.,* 2017). Briefly, 8 g of PAM was dissolved in 40 ml of double deionized water. The homogeneous, clear solubility was attained through rigorous magnetic stirring over the magnetic stirring plate for 30 minutes at 40 °C. Afterwards the solution was transferred to a 100 ml Teflon lined autoclave reactor. This reactor was sealed in a stainless steel case and placed in an electric oven for hydrothermal treatment at 270 °C for 24 hours. Following incubation, the reactor was left to cool down to room temperature. The formation of the yellow tinted solution was an indication that the formed product contains carbon quantum dots. The pH was then adjusted to 7 to ensure optimum use in electrochemical biosensor systems.

2.4 Purification of C-dots

For purification of yellow C-dots solution from the impurities of unreacted precursor, the C-dots solution was filtered through a syringe-filter with pore size 0.45 µm. For further purification, filtered C-dots solution was subjected to dialysis using a 4 kDa dialysis tube, suspended in phosphate buffered saline (PBS, pH 7.4, 100 ml) for 3 days. In this way, the unbound charged particles and other impurities were removed with pH maintained at 7. The samples prepared were stored at 4°C until further use.

2.5 Construction of C-dips

Chromatography paper (Whatman No.1) was cut into circles of 0.5 mm diameter. Here, 4 µL of the C-dots solution was added to the paper surface. Then 4 µL of serially diluted samples of iron and copper solutions were added onto a separate reaction zone of C-dots coated papers. After each addition, paper sensors were air dried for 10 minutes.

2.6 Colorimetric sensing of Iron and Copper using C-dots-based C-dips

The colorimetric sensing of iron and copper was carried out at room temperature using C-dots-based C-dips. In aliquot of the as-synthesized solution having C-dots NPs, iron and copper samples were added in the concentration range of 1×10^{-4} to 1×10^{-2} M. After stabilizing the mixture for few minutes, the quantification of corresponding concentration was done by observing the change in absorbance. The absorbance of the reaction mixture was measured using a spectrophotometer at a wavelength of 280 nm. On the other hand, C-dips coated with different concentrations of C-dots solution (10-50 µl) were used to record the change in colorimetric output against the different percentages of copper and iron samples (1M, 2 µl). After 5 minutes of air-drying and stabilizing the reagent and sample, the visible color change was captured using an 18-megapixel digital camera while the fluorescence change was photographed under UV using a Smartphone camera. The images were analyzed for color intensity using the image analysis program, ImageJ by the National Institute of Health (NIH), USA. Later the mean intensity values of different concentrations were calculated to generate a calibration curve.

3. Results and Discussion

3.1 Chemical and compositional characteristics of carbon nanodots (C-dots)

The as-synthesized C-dots were characterized for their chemical and compositional characteristics using XRD, Raman and XPS analysis. Figure 1 shows the corresponding XRD and Raman spectrum obtained for C-dots. In the case of XRD, a broad shoulder near 21 degrees is apparent, confirming the amorphous nature of formed C-dots. The Raman spectra consist of two bands near 1300 and 1600 cm^{-1}, which are typical D and G bands of carbon (Liu *et al.*, 2019). As no un-related peaks appear, it could be anticipated that the formed C-dots are pure in composition. Figure 2 shows the XPS analysis of C-dots. As seen, the survey spectra consist of typical C, O and N binding energy peaks. The high-resolution C1 spectra could further be integrated into three bands associated with C=O (288.5 eV), C=C (284.0 eV), and C-N/C-O (286.0 eV) bands, whereas O1s spectra contain O-C and O=C binding energies near 531.8 eV and 533.6 eV respectively. The N1s spectra possessed N-C and N-H bonds near 399.1 eV and 401 eV respectively. These bands appear as a consequence of nitrogen-functionality present in PAM which, subsequent to the hydrothermal treatment, becomes part of C-dots enhancing their fluoresces properties (Liu *et al.*, 2017). As-synthesized PAM precursor-based C-dots exhibited yellow color (Figure 3(c)) and when C-dots solution was placed under UV light, a bright blue color was observed (Figure 3(d)) reflecting its size to be <10 nm. The TEM images of the as-synthesized C-dots are shown in Figure 3(a, b). As observed, the C-dots have no fusion between the particles and the average size of C-dots was estimated to be about 10-20 nm. The UV-Vis spectroscopy confirms the typical absorption peak near 280 nm (Figure 3(c)), whereas a fixed emission peak 565 nm was observed in the corresponding PL spectra of C-dots (Figure 3(d)).

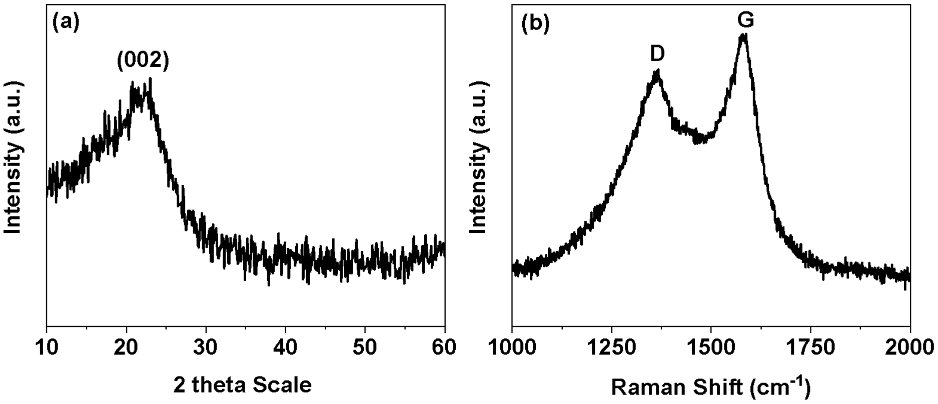

Fig. 1. The compositional characterization of C-dots prepared using PAM as a precursor (a) XRD pattern (b) The corresponding Raman spectra with representative D and G bands

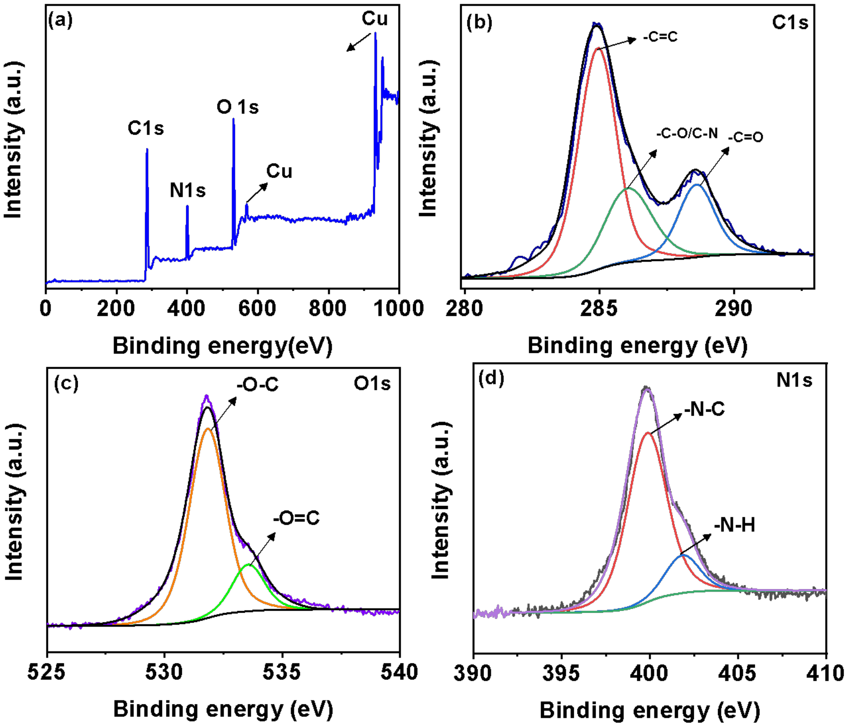

Fig. 2. The XPS analysis (a) survey spectrum (b) C1s (c) O1s (d) N1s high-resolution peak-fitting profiles of C-dots prepared using PAM as precursor using hydrothermal treatment

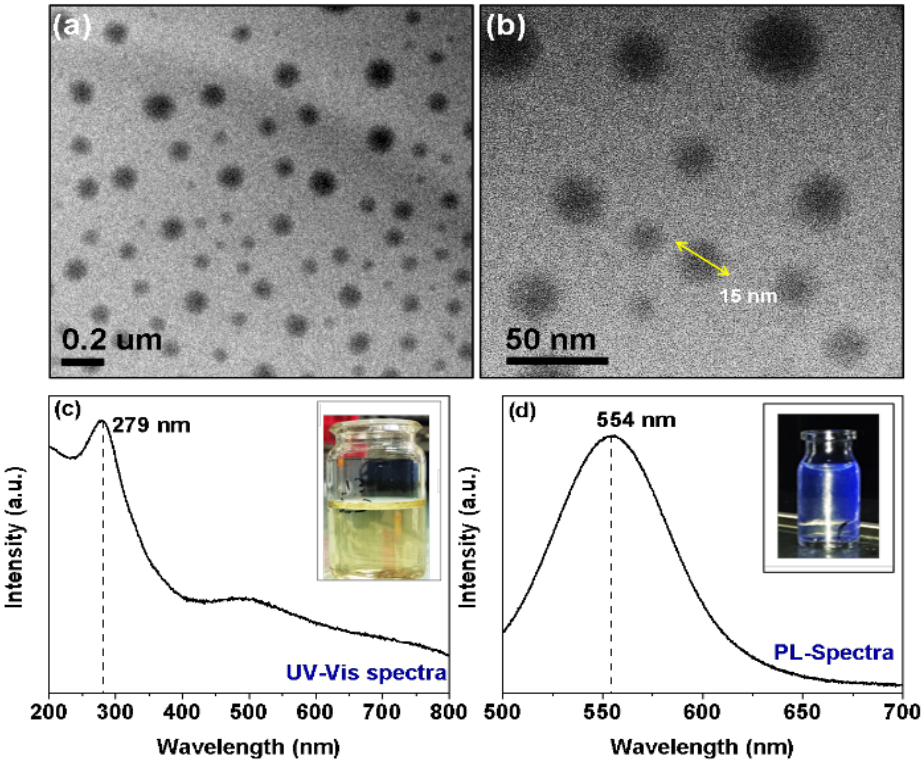

Fig. 3. The TEM images: (a) low-magnification, (b) high magnification showing dispersive nature of C-dots, (c) the corresponding UV-spectra with representative absorbance band near 250 nm; inset shows the color yellowish C-dots formed by hydrothermal route, (d) the PL spectra with inset showing the bright blue color of C-dots under UV-light

3.2 Colorimetric sensing of Iron and Copper Ions

The colorimetric detection of clinically important metal ions was carried out by configuring C-dots into simple nano-C-dips using Whatman No.1 filter paper tailored into spherical C-dips. These C-dips were initially soaked with specific dilutions of as-prepared C-dots and color intensity was calibrated by measuring the color intensity using imageJ. Figure 4(a) shows the photo visualization of the prepared C-dips soaked with different volumes of C-dots and their visible color change against the different percentages of Fe^{3+} (0.1 M, 2 μL). In reference to the blank (C-dips without Fe^{3+}), a strong color change was observed from white/pale yellow to brown as shown in the top row of Figure 4(a). Since, the visible change of color was noticed with every dilution of C-dots and Fe^{3+} ions which is in accordance with previous studies (Yoo *et al.*, 2019), the C-dots could be used as a natural label-free indicator of Fe^{3+}. This is promising for developing on-site fast yet disposable sensors.

The analytical quantification requires a more sophisticated approach and thus, pixel intensity measurement was considered to evaluate the color change-intensity which provides more reliable quantification compared to naked-eye detection. Here, the blank C-dip is considered bright as the pixel analysis confirms its intensity compared to the C-dips soaked in

Fe^{3+} ions of different concentrations. As seen in Figure 4(b) the maximum color-intensity could be achieved with an increase in both C-dots volume and percentage of Fe^{3+} in the system. This, direct quantification of metal ions such as Fe^{3+} could be achieved using this linear relationship. In regard to the maximum intensity, change is essential to develop as a reliable quantification method. As C-dots are known for their fluoresces properties, thus, further quantification was carried under UV-light. In this case, Fe^{3+}, Fe^{2+} and Cu^{2+} were taken as standard metal ions for detection. These metal ions with their strong adsorption capability towards C-dots were expected to quench the fluoresce emission of C-dots soaked C-dips, due to binding between C-dots and Fe^{3+}. This quenching could be quantified using pixel analysis and thus easy quantification of clinically important metal ions could be anticipated. Figure 5 (a-c) shows the calibration curves plotted for the change in fluoresce intensity (towards dark) of C-dips (soaked with C-dots (4 µL)) post addition of metal ions (Fe^{3+}, Fe^{2+} and Cu^{2+}) in the concentration range of 1×10^{-4} to 1×10^{-2} M. As evident, the best quenching was observed for iron metal ions (Fe^{3+} and Fe^{2+}), whereas Cu^{2+} had a relatively poor response. The LOD from the paper-based C-dips were estimated to be 3.89×10^{-5} µM, 4.65×10^{-5} µM and 6.7×10^{-5} µM for Fe^{3+}, Fe^{2+} and Cu^{2+} respectively. The generalized mechanism for rapid colorimetric detection of Fe^{3+} using carbon nanodots-based C-dips is illustrated in Figure 5(d). This indicated that the paper-based sensor had more effective and better performance compared to a solution-based sensor with the additional advantage of disposability without any environmental concerns. Furthermore, fabrication of paper-based assays using functionalized C-dots can provide a more sensitive and specific way to screen various analytes in reduced time and technical resources.

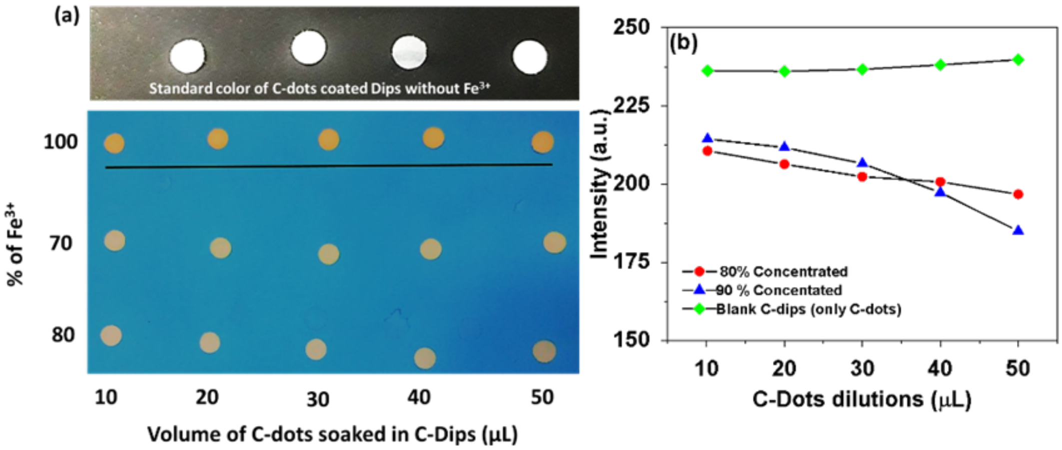

Fig. 4. (a) The naked eye color change observed after specific percentage of Fe^{3+} are introduced over C-dips immersed with different dilutions of C-dots concentrations (10 to 50 µL) in reference to C-dots with no target analyte (blank), (b) the corresponding pixel-intensity measurement, the y-axis represents the color intensity of data point for samples from a paper-based assay, while the X-axis represents C-dots concentration, showing maximum intensity inhibition obtained with 50 µL of C-dots and % Fe^{3+} ions solution

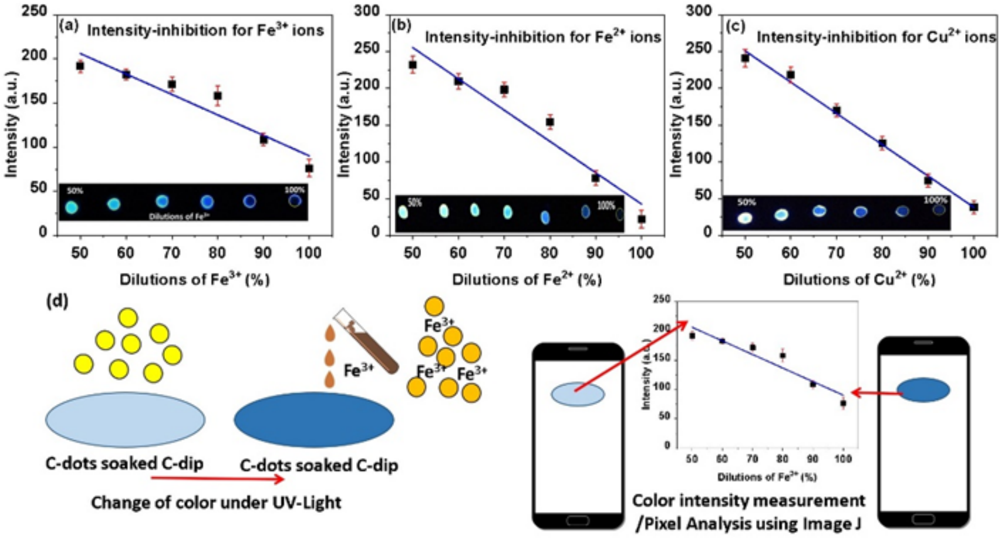

Fig. 5. Analytical Quantification of (a) Fe^{3+} (b) Fe^{2+} (c) Cu^{2+} using standard C-dips (d) a generalized schematic illustrating the color-change process and quantification approach of the prepared C-dips

4. Conclusion

The sensitivity and specificity of paper-based diagnostic assays can further be enhanced by employing nanomaterials. In this study, we have demonstrated the use of C-dots-based paper sensors for the detection of iron (Fe^{2+}, Fe^{3+}) and copper (Cu^{2+}). The paper sensor showed naked eye visible color change from white/pale yellow to brown for iron only while significant quenching of C-dots was observed under UV both for iron and copper. The Fe^{3+}, Fe^{2+} and Cu^{2+} could be detected sensitively up to 3.89×10^{-5} µM, 4.65×10^{-5} µM and 6.7×10^{-5} µM reflecting the efficiency of C-dips for analytical performance with the additional advantage of disposability without any environmental concerns. Such sensors can be modified to analyze not only iron and copper in human serum samples but also for other disease related analytes as a low-cost alternative to traditional sensing techniques in resource-limited settings.

ACKNOWLEDGEMENTS

Authors would like to thank to Dr. Sadia Zafar Bajwa, Principal Scientist, Industrial Biotechnology Division, NIBGE, Faisalabad, Pakistan for her valuable suggestions in this study.

References

Adnan, S., Hussain, N., Abbas, M., Soomro, R., Saand, M., Awan, F., Avci, A., Pehlivan, E. & Bajwa, S. (2019) Enzyme-free colorimetric sensing of glucose using l-cysteine functionalized silver nanoparticles. SN Applied Sciences*,* 1.

Chaiyo, S., Siangproh, W., Apilux, A. & Chailapakul, O. (2015) Highly selective and sensitive paper-based colorimetric sensor using thiosulfate catalytic etching of silver nanoplates for trace determination of copper ions. Analytica Chimica Acta, 866: 75-83.

Chan, K.K., Yang, C., Chien, Y.H., Panwar, N. & Yong, K.T. (2019) A facile synthesis of label-free carbon dots with unique selectivity-tunable characteristics for ferric ion detection and cellular imaging applications. New Journal of Chemistry, 43: 4734-4744.

Chen, Y., Sun, X., Pan, W., Yu, G. & Wang, J. (2020) Fe3+-Sensitive Carbon Dots for Detection of Fe3+ in Aqueous Solution and Intracellular Imaging of Fe3+ Inside Fungal Cells. Front. Chem, 7.

Gao, X., Lu, Y., He, S., Li, X. & Chen, W. (2015) Colorimetric detection of iron ions (III) based on the highly sensitive plasmonic response of the N-acetyl-l-cysteine-stabilized silver nanoparticles. Analytica Chimica Acta, 879: 118-125.

Guo, J.F., Huo, D.Q., Yang, M., Hou, C.J., Li, J.J., Fa, H.B., Luo, H.B. & Yang, P. (2016) Colorimetric detection of Cr (VI) based on the leaching of gold nanoparticles using a paper-based sensor. Talanta, 161: 819-825.

Lee, V.B.C., Mohd-Naim, N.F., Tamiya, E. & Ahmed, M.U. (2018) Trends in Paper-based Electrochemical Biosensors: From Design to Application. Anal Sci, 34: 7-18.

Liu, G., Li, B., Liu, Y., Feng, Y., Jia, D. & Zhou, Y. (2019) Rapid and high yield synthesis of carbon dots with chelating ability derived from acrylamide/chitosan for selective detection of ferrous ions. Applied Surface Science, 487: 1167-1175.

Liu, Y., Zhou, Q., Yuan, Y. & Wu, Y. (2017) Hydrothermal synthesis of fluorescent carbon dots from sodium citrate and polyacrylamide and their highly selective detection of lead and pyrophosphate. Carbon, 115: 550-560.

Martinez, A.W., Phillips, S.T., Butte, M.J. & Whitesides, G.M. (2007) Patterned paper as a platform for inexpensive, low-volume, portable bioassays. Angew Chem Int Ed Engl, 46: 1318-20.

Martinez, A.W., Phillips, S. T., Carrilho, E., Thomas, S.W., Sindi, H. & Whitesides, G.M. (2008a) Simple telemedicine for developing regions: camera phones and paper-based microfluidic devices for real-time, off-site diagnosis. Anal Chem, 80: 3699-707.

Martinez, A.W., Phillips, S.T. & Whitesides, G.M. (2008b) Three-dimensional microfluidic devices fabricated in layered paper and tape. Proc Natl Acad Sci U S A, 105: 19606-11.

Mirabi, A., Rad, A. S. & Ahmadizadeh, S. (2019) Graphene Oxide Enhances SBA-15 Ability Towards Preconcentration as well as Determination of Barbiturate Drug in Real Samples. Kuwait Journal of Science, 46: 49-57.

Namdari, P., Negahdari, B. & Eatemadi, A. (2017) Synthesis, properties and biomedical applications of carbon-based quantum dots: An updated review. Biomedicine & Pharmacotherapy, 87: 209-222.

Nishat, S., Awan, F.R. & Bajwa, S.Z. (2019) Nanoparticle-based Point of Care Immunoassays for in vitro Biomedical Diagnostics. Anal Sci, 35: 123-131.

Piyanan, T., Athipornchai, A., Henry, C.S. & Sameenoi, Y. (2018) An Instrument-free Detection of Antioxidant Activity Using Paper-based Analytical Devices Coated with Nanoceria. Analytical Sciences, 34: 97-102.

Priyadarshini, E. & Pradhan, N. (2017) Gold nanoparticles as efficient sensors in colorimetric detection of toxic metal ions: A review. Sensors and Actuators B: Chemical, 238: 888-902.

Shah, H., Xin, Q., Jia, X. & Gong, J.R. (2019) Single precursor-based luminescent nitrogen-doped carbon dots and their application for iron (III) sensing. Arab. J. Chem, 12: 1083-1091.

Siqueira, J.R. & Oliveira, O.N. (2016) Carbon-Based Nanomaterials. In: Da Roz, A.L., Ferreira, M., De Lima Leite, F. & Oliveira, O.N. (Eds.) Nanostructures, Pp. 233-249. William Andrew Publishing.

Sun, X. & Lei, Y. (2017) Fluorescent carbon dots and their sensing applications. TrAC Trends in Analytical Chemistry, 89: 163-180.

Tan, S.C., Chin, S.F. & Pang, S.C. (2017) Disposable Carbon Dots Modified Screen Printed Carbon Electrode Electrochemical Sensor Strip for Selective Detection of Ferric Ions. J. Sens, 2017: 7576345.

Tuerhong, M., Xu, Y. & Yin, X.B. (2017) Review on Carbon Dots and Their Applications. Chinese J. Anal. Chem, 45: 139-150.

Kumar, V.V., Anbarasan, S., Christena, L.R., Saisubramanian, N. & Anthony, S.P. (2014) Bio-functionalized silver nanoparticles for selective colorimetric sensing of toxic metal ions and antimicrobial studies. Spectrochim. Acta A Mol. Biomol. Spectrosc, 129: 35-42.

Ye, J.S., Wen, Y., De Zhang, W., Gan, L.M., Xu, G. Q. & Sheu, F.S. (2004) Nonenzymatic glucose detection using multi-walled carbon nanotube electrodes. Electrochemistry Communications, 6: 66-70.

Yoo, D., Park, Y., Cheon, B. & Park, M.H. (2019) Carbon Dots as an Effective Fluorescent Sensing Platform for Metal Ion Detection. Nanoscale Research Letters, 14: 272.

Zhao, A., Chen, Z., Zhao, C., Gao, N., Ren, J. & Qu, X. (2015) Recent advances in bioapplications of C-dots. Carbon, 85: 309-327.

Submitted: 30/04/2021
Revised: 25/04/2022
Accepted: 15/06/2022
DOI: 10.48129/kjs.13997